Applied Acoustics 114 (2016) 118–124

Contents lists available at ScienceDirect

Applied Acoustics

journal homepage: www.elsevier.com/locate/apacoust

Flexural wave suppression by an acoustic metamaterial plate

Ting Wang [a,b], Mei-Ping Sheng [a], Zhi-Wei Guo [a], Qing-Hua Qin [b,*]

[a] School of Marine Science and Technology, Northwestern Polytechnical University, Xi'an, Shaanxi 710072, PR China
[b] College of Engineering and Computer Science, The Australian National University, ACT 2600, Australia

ARTICLE INFO

Article history:
Received 1 November 2015
Received in revised form 22 July 2016
Accepted 22 July 2016

Keywords:
Metamaterial plate
Lateral local resonance
Flexural band gaps
Wave propagation

ABSTRACT

A new acoustic metamaterial plate is presented for the purpose of suppressing flexural wave propagation. The metamaterial unit cell is made of a plate with a lateral local resonance (LLR) substructure which consists of a four-link mechanism, two lateral resonators and a vertical spring. The substructure presents negative Young's modulus property in certain frequency range. We show theoretically and numerically that two large low-frequency band gaps are obtained with different formation mechanisms. The first band gap is due to the elastic connection with the foundation while the second is induced by the lateral resonances. Besides, four-link mechanisms can transform the flexural wave into the longitudinal vibration which stimulates the lateral resonators to vibrate and to generate inertial forces for absorbing the energy and thus preventing the wave propagation. Frequency response function shows that damping from the vertical spring has little influence on the band gaps, although the damping can smooth the variation of frequency response (see the dotted line in Figs. 10 and 11). Increasing the damping of the lateral resonators may broaden the second band gap but deactivate its effect. This study provides guidance for flexibly tailoring the band characteristics of the metamaterial plate in noise and vibration controls.

1. Introduction

Continuum structures like beams, plates and shells are the most widely preferred elements in engineering applications such as the construction of the buildings, experimental tables and some large ships and submarines. Controlling the propagation of flexural waves in continuum structures is one of the most important issues in the safety and stability of such engineering structures [1]. An example is a submarine in service, which may radiate energy to the surroundings, thereby exposing its position and jeopardising safety. Since flexural wave is the main wave type for radiation, suppressing flexural waves is a vital safety issue. Moreover, in many experiments, vibration of the experimental table can influence the accuracy of results. In this situation, propagation of the flexural wave should be stopped. With the unique wave-blocking properties of metamaterial, studies have been devoting themselves to apply these novel properties for the control of wave propagation. Early studies [2] of wave propagation in metamaterial were mainly focused on dispersion analyses of longitudinal wave and band gaps of simple lattices. Huang et al. proposed different types of metamaterial lattices for blocking longitudinal wave propagation [3–6]. Zhang et al. disentangled longitudinal and shear elastic waves by neo-Hookean soft devices [7]. These studies are focusing on in-plane waves and still remote from engineering applications but provide guidance for metamaterial design.

In recent years, extensive investigations have been conducted on preventing flexural wave propagation within continuum structures in different structural configurations. It has been theoretically and numerically predicted that attaching absorbers to a beam or plate to construct a metamaterial could constrain flexural wave propagation [8–14], which is classified as 'Site-City Effect' in geophysics [15,16], and inserting absorbers into a sandwiched beam or plate [17–21] may also prevent such propagation. Further, beams and plates with perforated holes filled with a membrane and a mass in the centre exhibit novel properties for controlling flexural wave, but at the expense of decreasing strength [22–25], as with this method, the stiffness of the metamaterial has been dramatically decreased. The resonators mentioned above are all directly attached to continuum structures and vibrate in the perpendicular direction to the continuum structure. Only few researchers have investigated mechanisms for transforming the flexural wave into another direction and blocking the wave propagation in the new direction, e.g. Chesnais et al. [26,27] for reticulated structures.

The LLR substructure proposed by Huang and Sun [5,28] is composed of a four-link mechanism, two lateral resonators and a vertical spring. It exhibits an unusual frequency-dependent effective

* Corresponding author.
E-mail address: qinghua.qin@anu.edu.au (Q.-H. Qin).

http://dx.doi.org/10.1016/j.apacoust.2016.07.023
0003-682X/

Young's modulus and transforms the vibration to another direction. Huang and Sun [20] showed that the periodic arrangement of the LLR substructure could attenuate the longitudinal wave propagation through the wave transformation mechanism. Recently, their group extended the lumped structure to a continuum structure based on beam elements [29]. However, investigation is still limited to longitudinal wave attenuation. Yet, as mentioned, the flexural wave is the main energy storage type. Controlling the flexural wave using the LLR substructure has great potential for engineering applications. To our knowledge, combination of the classical continuum structure with the lumped LLR substructure to form an acoustic metamaterial has not been discussed.

In this paper, we propose an acoustic metamaterial plate with LLR substructures for flexural wave suppression. To investigate the mechanism of the transformation of the waves, the dynamic characteristics of an LLR substructure are analysed in Section 2. The combination of the LLR and continuum plate is theoretically modelled in Section 3, including the analysis of dispersion surfaces and effective mass density. Finite element analysis is conducted in Section 4 to investigate the flexural wave propagation and damping effects. The outcome is expected to provide helpful guidance for generating multiple low frequency band gaps in flexural wave suppression and noise absorption.

2. Configuration of the negative Young's modulus substructure

The LLR substructure analysed here is different from that detailed by Huang and Sun [5]. As shown in Fig. 1, the LLR substructure consists of four-link mechanism, two lateral resonators and a vertical spring. The four-link mechanism is joined to the ground and a harmonic force $F = \tilde{F}e^{-j\omega t}$ is applied to the other end, which plays the role of transforming the vertical vibration into horizontal vibration. The lateral resonators with spring and mass constants of k_2 and m_2 vibrate only in the horizontal direction. The vertical spring k_1 moves vertically. The governing equation for this lumped system is

$$F = k_1 w + \frac{L}{D} k_2 (u - v) \tag{1}$$

$$m_2 \frac{\partial^2 u}{\partial t^2} = k_2 (v - u) \tag{2}$$

where w, u and v represent the displacement of the vertical point of the truss, the lateral mass and the horizontal point of the truss, respectively. L and D are the vertical and horizontal length of the four-link mechanism. Assuming the vibration is small, relationship of displacements v and w can be written as

$$v = -\frac{L}{2D} w \tag{3}$$

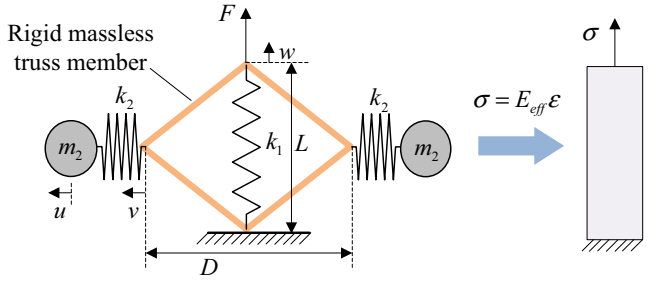

Fig. 1. Configuration of the negative Young's modulus inclusions and its effective continuum model.

In our analysis, the displacement fields are assumed in the harmonic form

$$w = \tilde{w}e^{-i\omega t}, u = \tilde{u}e^{-i\omega t} \tag{4}$$

Substitution of Eqs. (3) and (4) into Eqs. (1) and (2) yields the force-displacement relation as

$$\tilde{F} = \left(k_1 + \frac{1}{2}\left(\frac{L}{D}\right)^2 \frac{k_2\omega^2}{\omega^2 - \omega_0^2}\right)\tilde{w} \tag{5}$$

where $\omega_0 = \sqrt{k_2/m_2}$. Using a continuum elastic solid to represent the lumped system with the cross section area A, the stress-strain relation is defined as

$$\sigma = E_{eff}\varepsilon \tag{6}$$

with $\sigma = F/A$ and $\varepsilon = w/L$ respectively. E_{eff} is the effective Young's modulus of the continuum system. Denoting that $E_0 = k_1 L/A$, the normalized effective Young's modulus is calculated by

$$\frac{E_{eff}}{E_0} = 1 + \frac{k_2}{2k_1}\frac{\omega^2}{\omega^2 - \omega_0^2}\left(\frac{L}{D}\right)^2 \tag{7}$$

in which $k_1 = 1 \times 10^4$ N/m, $m_2 = 0.003$ kg, $k_2 = 0.5 \times 10^4$ N/m, $L = 0.02$ m, and $D = 0.01$ m.

Fig. 2 shows the effective Young's modulus of LLR substructure as a function of frequency. It is obvious that from 145 Hz to 205 Hz, the effective Young's modulus is negative whereas in other ranges it remains positive. At the frequency of 205 Hz, the effective Young's modulus is unbounded because of the resonance of the lateral local resonators. Around the resonance frequency, waves can be effectively attenuated, according to the results of Huang and Sun [5].

With the above analysis of the LLR substructure, we can see that the vibration direction of the stimulus F and that of the LLR substructure u are different. The four-link mechanism can transform the vertical vibration into longitudinal vibration, thus controlling the wave in a unique way. This transformation can be used to design different absorbers and isolators for wave suppression. Considering that flexural waves in beams and plates are the main energy type, the LLR substructure is suitable for the design of acoustic metamaterials for wave attenuation.

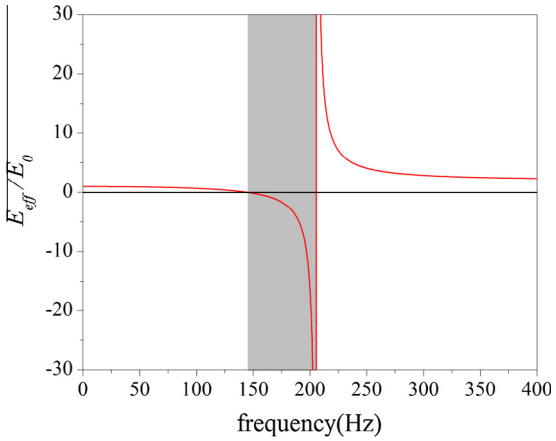

Fig. 2. The effective Young's modulus versus frequency.

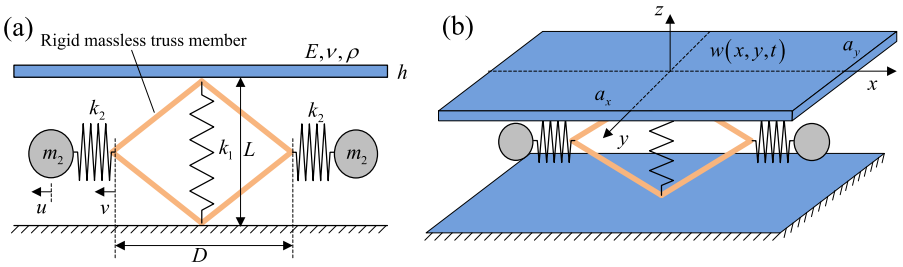

Fig. 3. The unit cell of the metamaterial plate: (a) front view, (b) perspective view.

3. Wave suppression within a continuous metamaterial plate

3.1. Theoretical derivation

Fig. 3 shows a unit cell of a metamaterial plate which consists of a rectangular homogeneous plate and a LLR substructure with one end connected to the plate, the other end to the ground. Such configuration of the metamaterial seems like a homogeneous plate resting on an elastic foundation [30]. The plate's edge lengths along the x and y directions are a_x and a_y, respectively. k_1 represents the vertical spring stiffness, and k_2 and m_2 are the lateral spring and mass constants. For the four-link mechanism, the vertical distance and horizontal distance are L and D, respectively. The unit cell of the metamaterial plate is a 2-DOF system with the plate vibrating vertically and the local resonators oscillating horizontally.

With the assumption of small displacement, we have

$$v(t) = -\frac{L}{2D} w_0(t) \tag{8}$$

where $v(t)$ is the lateral displacement of the four-link mechanism. $w_0(t)$ is the central flexural displacement of the plate. The governing equation for flexural wave propagation through the upper thin plate [31,32] is

$$\rho h \frac{\partial^2 w(x,y,t)}{\partial t^2} = -\tilde{D}\nabla^2\nabla^2 w(x,y,t) + q(x,y,t) \tag{9}$$

where $\nabla^2 = (\partial^2/\partial x^2 + \partial^2/\partial y^2)$, $\tilde{D} = Eh^3/12(1-\nu^2)$ denote the plate's flexural rigidity, with E, ν representing the Young's modulus and Poisson's ratio of the plate, respectively. ρ and h are the plate's mass density and thickness, respectively. $q(x,y,t)$ is the force applied to the unit cell. For the system, the force equilibrium equations are

$$q(0,0,t) = -nk_1 w_0(t) - 2k_2 n \frac{L}{2D}(u(t) - v(t)) \tag{10}$$

$$m_2 \frac{\partial^2 u(t)}{\partial t^2} = k_2(v(t) - u(t)) \tag{11}$$

where $n = 1/a_x a_y$, and $u(t)$ is the horizontal displacement of the lateral mass m_2. From Eqs. (9)–(11), it can be seen that $w(x,y,t)$ is a global variable, while $v(t)$, $w_0(t)$ and $u(t)$ are all local variables. And $v(t)$ can be represented by $w_0(t)$, as Eq. (8).

By analogy of Eqs. (1), (2) and Eqs. (10), (11), we have

$$q(0,0,t) = -nE_{eff} w_0(t) = -Kw_0(t) \tag{12}$$

with $K = E_{eff}/a_x a_y$, the bulk modulus of the metamaterial plate treated as a homogeneous layer, and the performance is the same as that described in Section 2. And Eq. (9) can be written as

$$\rho h \frac{\partial^2 w(x,y,t)}{\partial t^2} = -\tilde{D}\nabla^2\nabla^2 w(x,y,t) - Kw_0(t) \tag{13}$$

Based on the plane wave propagation and the periodicity of the unit cell within the infinite metamaterial plate, the displacement of the plate $w(x,y,t)$ can be expressed in the form

$$w(x,y,t) = We^{i(\kappa_1 x + \kappa_2 y - \omega t)} = w_0(t)e^{i(\kappa_1 x + \kappa_2 y)} \tag{14}$$

where κ_1 and κ_2 are the wavenumbers along the x and y directions with $\kappa_1 = 2\pi/\lambda_1$, $\kappa_2 = 2\pi/\lambda_2$. λ_1 and λ_2 are the corresponding wavelengths. ω is the wave frequency. Setting

$$\boldsymbol{\kappa} = (\kappa_1, \kappa_2), \kappa^2 = |\boldsymbol{\kappa}|^2 = |\kappa_1^2 + \kappa_2^2| \tag{15}$$

Substitution of Eqs. (14), (15) into (13) yields

$$(\tilde{D}\kappa^4 + K - \rho h\omega^2) w_0 = 0 \tag{16}$$

And the dispersion relation can be obtained by setting the coefficient of Eq. (16) to 0.

$$\kappa^2 = \pm \frac{\omega}{\sqrt{\tilde{D}}} \sqrt{h\left(\rho - \frac{K}{\omega^2 h}\right)} \tag{17}$$

When the metamaterial plate is treated as a homogeneous plate, the effective mass density is identified as

$$\rho_{eff} = \rho\left(1 - \frac{K}{\rho\omega^2 h}\right) \tag{18}$$

Assuming that pairs of wave vector are given, through Eq. (17), the angular frequency can be yielded the relationship among ω, κ_1 and κ_2. Since the unit cell is symmetry referred to the central origin, the range of the wave vectors should be $\kappa_1 \in [0, \pi/a_x]$, $\kappa_2 \in [0, \pi/a_y]$.

Fig. 4 shows the band gaps of the unit cell, with parameters used in the calculation as: the unit size $a_x = 0.02$ m, $a_y = 0.02$ m, the plate's thickness $h = 0.005$ m, the Young's modulus $E = 2.1 \times 10^{11}$ Pa, the Poisson's ratio $\nu = 0.3$, the mass density $\rho = 7800$ kg/m^3, the vertical spring stiffness $k_1 = 1 \times 10^4$ N/m, the lateral spring and mass constants $k_2 = 0.5 \times 10^4$ N/m and $m_2 = 0.003$ kg, the vertical and lateral distances of four-link mechanism $L = 0.02$ m, $D = 0.01$ m.

Several interesting phenomena are found from Fig. 4, as follows. (1) There are two dispersion surfaces, and two band gaps exist in the metamaterial plate, 0–103 Hz and 205 Hz–253 Hz, respectively. Both these band gaps are significantly useful in engineering applications in which flexural waves must not propagate through the composite. (2) The formation mechanisms of the two band gaps differ. There exists a pivotal frequency for the Winkler-type foundation system [33], and because of the restraints of elastic foundation, which affects the integrality of the system and decrease the flexural stiffness, the first band gap is formed. Owing to the elastic support of the vertical spring, which forms a Winkler-type system, vibration is blocked within the first band gap. For the lateral resonators, the resonance occurs at 205 Hz and the second band gap begins at 205 Hz. This shows that the four-link mechanism can transform the flexural wave to a longitudinal wave which stimulates the lateral resonators to vibrate and then generate inertial forces to counterbalance the shear forces and thus absorb the wave energy. (3) The transformation is related to the ratio L/D, which means that the ratio L/D significantly affects the

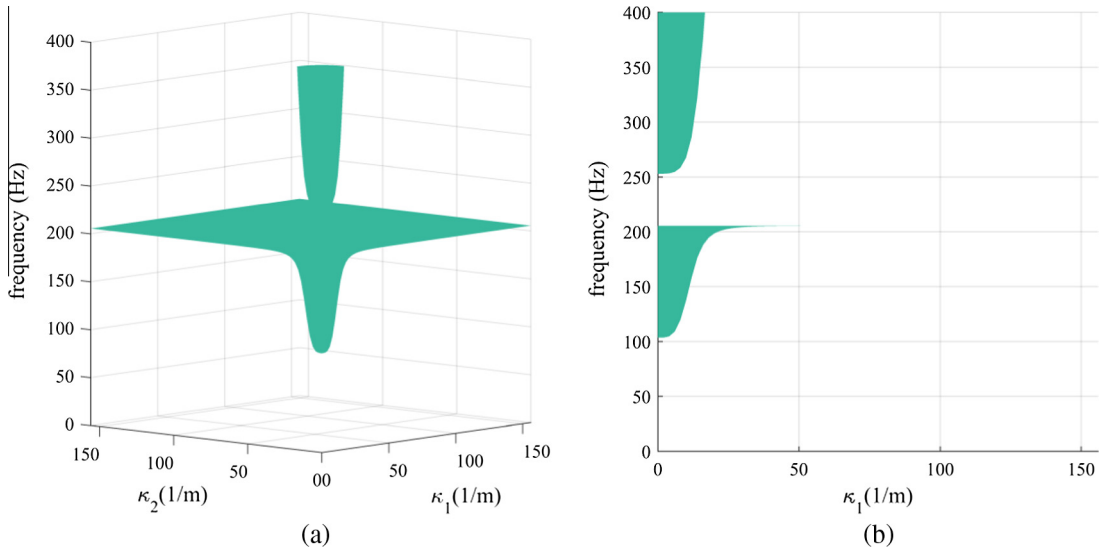

Fig. 4. Dispersion surfaces of the metamaterial plate: (a) perspective view, (b) front view.

transformation from flexural to longitudinal vibration. The effect of the ratio L/D on the band gaps is discussed in Section 3.2. (4) The metamaterial plate with LLR substructures provides a flexible structure configuration that can generate multiple band gaps for flexural vibration suppression and wave absorption.

3.2. Effect of the ratio L/D on the band gaps

As indicated above, the transformation from flexural wave to longitudinal wave is significantly affected by the geometry parameter of the four-link mechanism. In this section we examine the effect of the ratio L/D on the transformation process. It should be mentioned that in the analysis in Section 3.1, the ratio of L/D is set as 2. To study its effects on the interval of the band gaps, the ratio L/D is assumed to be between 0.5 and 2.5 with the incremental step being 0.2, where, the other parameters are kept constant. Results for the edges of the two band gaps are shown in Fig. 5.

It can be seen from Fig. 5 that the upper edge of the first band gap moves towards a lower frequency range, which means that the first band gap becomes narrower as the ratio L/D increases. For the second band gap, the lower edge remains the same because the lateral resonators remain unchanged, while the upper edge climbs to a higher frequency range, which means that the second band gap is broadened along with an increase in the ratio of L/D. Comparison of the slopes of upper edges between the first and second band gaps shows that the rate of increase of the second band gap is faster than the rate of decrease of the first band gap. The two band gaps can be flexibly tuned by varying the ratio L/D of the four-link mechanism with the other parameters unchanged.

3.3. Effective mass density

The effective mass density from Eq. (18) can be obtained as

$$\rho_{eff} = \rho\left(1 - \frac{K}{\rho\omega^2 h}\right) = \rho - \frac{nk_1}{h\omega^2} - \frac{1}{2}\frac{nk_2}{h\omega^2}\left(\frac{L}{D}\right)^2 - \frac{nk_2^2}{h\omega^2(m_2\omega^2 - k_2)}\frac{1}{2}\left(\frac{L}{D}\right)^2 \quad (19)$$

In the calculation, parameters are set the same as those in Section 3.1, and effective mass density of the metamaterial plate is shown in Fig. 6.

It is obvious from Fig. 6 that the effective mass density of the metamaterial plate becomes negative within the band gaps, and approaches to negative infinity at about 35 Hz and 205 Hz. The first infinity represents the counterbalance of the shear forces induced by plate vibration and the inertial forces of the vertical springs,

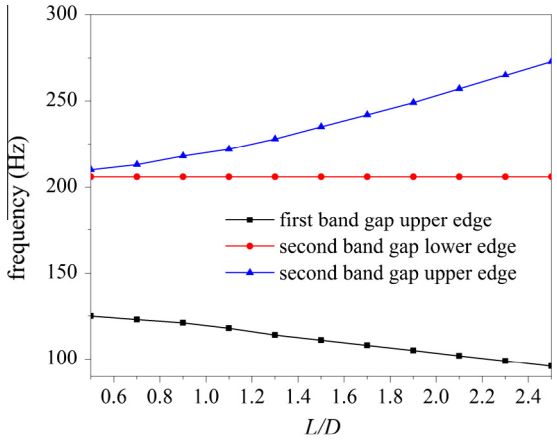

Fig. 5. Effect of L/D on band gaps.

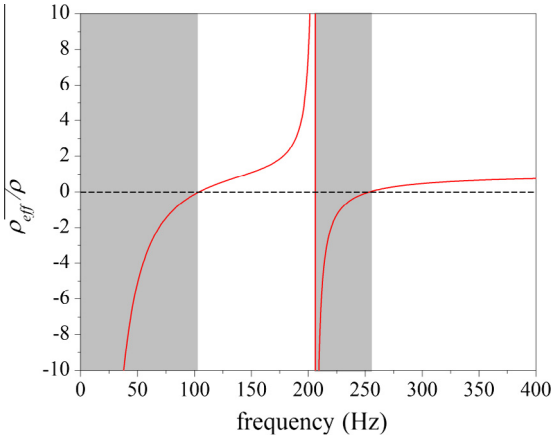

Fig. 6. Effective mass density of the metamaterial plate.

while the second infinity is attributable to the resonance of the lateral resonators.

The negative effective mass density in the band gaps also provides a good explanation of the flexural wave attenuation. Flexural vibration of the plate can be expressed as $w(x,y,t) = We^{i(\kappa_1 x+\kappa_2 y-\omega t)}$, and the flexural wave velocity is $c_f = -i\omega We^{i(\kappa_1 x+\kappa_2 y-\omega t)}$. Setting $C_f = -i\omega W$, the flexural wave velocity can be written as $c_f = C_f e^{i(\kappa_1 x+\kappa_2 y-\omega t)}$. From Eq. (17), the complete set of solution of $\boldsymbol{\kappa} = (\kappa_1, \kappa_2)$ should be given as

$$\boldsymbol{\kappa} = (\kappa_1, \kappa_2) \in \left\{ \pm\sqrt{\sqrt{\frac{h}{\bar{D}}\rho_{eff}\omega^2}}; \pm i\sqrt{\sqrt{\frac{h}{\bar{D}}\rho_{eff}\omega^2} } \right\} \tag{20}$$

Within ranges of the negative effective density, the wave vector takes the form

$$\boldsymbol{\kappa} = (\kappa_1, \kappa_2) \in \pm\{1; i\}\frac{1+i}{\sqrt{2}}\sqrt{\sqrt{\frac{h}{\bar{D}}|\rho_{eff}|\omega^2}} \tag{21}$$

Eq. (21) indicates that flexural waves are only attenuated when the density is negative (since $\boldsymbol{\kappa}$ only has imaginary part). That is, for a specific wave frequency, negative mass density results in complex wave numbers, i.e. $\kappa_1 = m_1 + im_2, \kappa_2 = n_1 + in_2$, with $m_1, m_2, n_1, n_2 > 0$ and real. Therefore, $w(x,y,t) = We^{-m_2 x - n_2 y}e^{-i(m_1 x+n_1 y+\omega t)}$ and $c_f = C_f e^{-m_2 x-n_2 y}e^{-i(m_1 x+n_1 y+\omega t)}$, both of which indicate that the flexural wave attenuates in an exponential form within the band gaps.

4. Finite element modelling and frequency response analysis of the metamaterial plate

4.1. Finite element modelling of the metamaterial plate

To simulate the performance of flexural wave suppression, the finite element method (FEM) [34,35] is used. The mechanical model of the metamaterial plate used for finite element analysis (FEA) as shown in Fig. 7 is employed to investigate the performance of flexural wave suppression of the four-link mechanism. In the analysis, some parameters of the metamaterial plate are: $L_x = 0.5$ m, $L_y = 0.2$ m (length along x, y directions), $h = 0.005$ m, $E = 210$ GPa, $v = 0.3$, $\rho = 7800$ kg/m^3 for the homogeneous plate; $k_1 = 1\times10^4$ N/m, $k_2 = 0.5\times10^4$ N/m, $m_2 = 0.003$ kg, $L = 0.02$ m, $D = 0.01$ m, $\sqrt{k_2/m_2}/2\pi = 205$ Hz for the LLR substructure.

Since the lateral masses vibrate in the x direction only, the inertial force due to acceleration for the homogenous plate can be neglected. A harmonic excitation force $F = F_0 e^{i\omega t}, F_0 = 100$ N is applied at the centre point of the left boundary of the plate. The upper plate is under free boundary condition, while the lower plate is nearly fastened to the ground by fixing its four edges to the ground. In this situation, the relationship of the displacements of lateral points and vertical points of the four-link mechanism is the same as that of the single substructure, and easier to analyse. The plate is built by using a four-node plate element SHELL 63 with four degrees of freedom at each node and meshed with mapped techniques. BEAM 188 with huge Young's modulus and tiny density is adopted to mimic the rigid massless link. MASS 21 and COMBIN 14 are the mass and spring elements with corresponding properties in the construction of the finite element model. The steady state response is examined through harmonic response analysis. In the construction of the finite element model, the FRF matrix can be derived as follows.

$$[M]\{\ddot{q}\} + [C]\{\dot{q}\} + [K]\{q\} = \{F\}, \tag{22}$$

$$\begin{aligned} \{F\} &= \{0, \cdots, 0, F_0 e^{i\omega t}, 0, \cdots, 0\}^T \\ \{q\} &= \{w_x, w_y, w_z, \ldots u_1, \ldots\} \end{aligned} \tag{23}$$

$$[H] = \left(-\omega^2[M] + i\omega[C] + [K]\right)^{-1} \tag{24}$$

$$\{q\} = [H]\{F\} \tag{25}$$

where $[M]$, $[C]$ and $[K]$ are the mass matrix, linear viscous damping matrix and the stiffness matrix of the finite element model. To obtain the $H_{r,cp}$ of node at specific points (the central point of the right boundary) with a harmonic excitation at the central point of the left boundary, the flexural displacement has been extracted, and by using Eq. (25),

$$H_{r,cp} = 20\log_{10}(|q|_{r,cp,w_z} F_0^{-1}) \tag{26}$$

The frequency response function (FRF) is plotted in Fig. 8 to show the band gap effect on propagation of flexural wave, damping is not included.

Fig. 8 demonstrates the FRF of the metamaterial plate under a harmonic excitation. The dashed line represents the response from the proposed metamaterial plate, while the solid line represents the response of plate without lateral resonators. It can be seen that when the LLR substructure is added to the metamaterial plates, a new broad band gap of the frequency range from 205 Hz to 253 Hz is generated, with almost no change in the first band gap because the flexural vibration has been transformed to longitudinal vibration by the four-link mechanism, which stimulates the resonance of the lateral mass, resulting in blocking the wave propagation. The numerical results show good consistency with the theoretical results.

To visualize the formation mechanism of the band gaps, the vibration modes are provided within different band gaps, as shown in Fig. 9.

Fig. 9(a) shows the vibration mode of the metamaterial plate at 82 Hz within the first band gap. It can be seen that for the first band gap, the plate vibrates vigorously around the excitation and part of the vertical springs are extensively stretched and com-

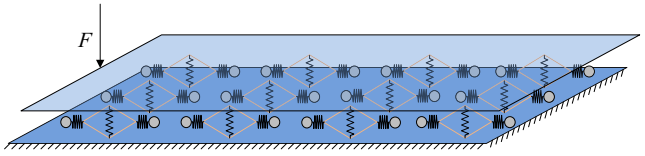

Fig. 7. Acoustic metamaterial plate with the bottom plate simply supported over the four edges.

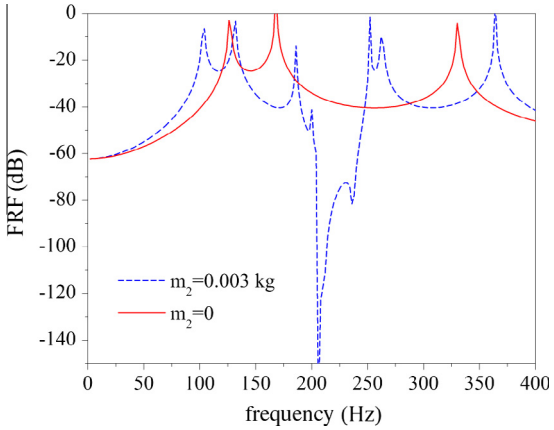

Fig. 8. Comparison of plate with and without the LLR substructure.

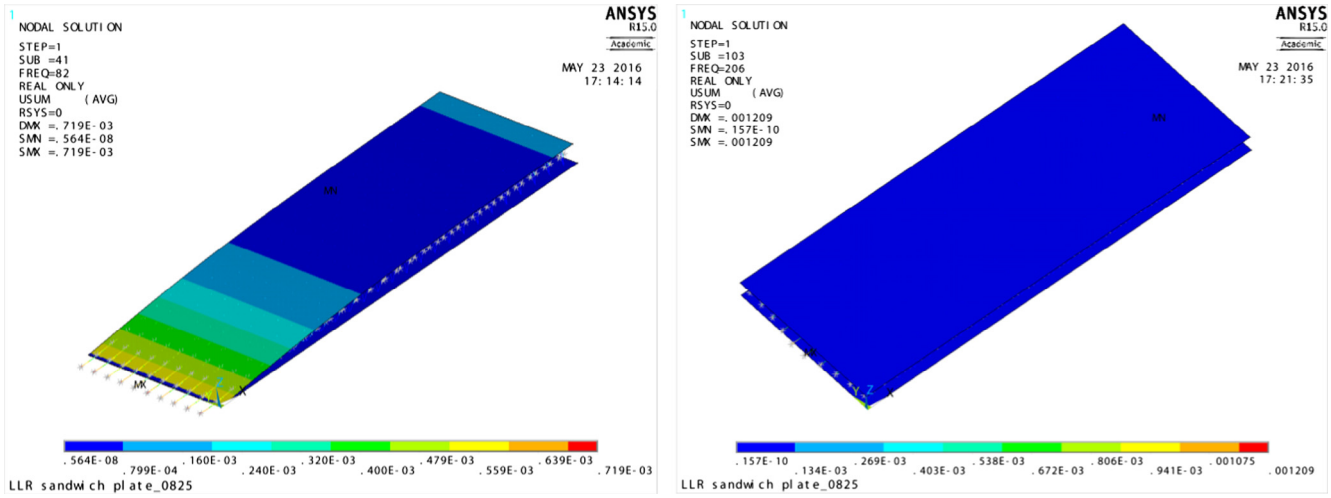

(a) mode shape at 82Hz (b) mode shape at 206Hz

Fig. 9. Vibration modes at different frequencies.

pressed. Flexural wave is partially transformed to the lateral resonators. Since the stimulus frequency is remote from the resonance of the resonators, the resonators only oscillate longitudinally and do not evoke wave suppression. Fig. 9(b) shows the vibration mode at 206 Hz, where the flexural vibration has been totally transformed to the lateral resonators. In this case, inertial forces generated by the lateral resonators are transferred through the four-link mechanism to counteract the shear forces induced by the plate flexural vibration, preventing the flexural wave from propagating.

4.2. Effect of linear viscous damping on band gaps

In practical engineering applications, damping is a significant factor that influences the dynamic behaviour of a structure. It should be mentioned that damping in an engineering structure can reduce the peak value and smooth the dynamic response curve. When a substructure with LLR is added to the plate, band gaps are formed in the system, resulting in changes to the wave responses. The influence of damping due to the presence of the LLR substructure is therefore critical and must be investigated. Viscous damping, though, is widely used in practical engineering, which can be modelled by a simple mechanical viscous damper (dashpot). In this article, linear viscous damping is chosen to analyse the effects on the band gaps. Linear viscous damping coefficients c_1 and c_2 are used to represent the linear damping of the vertical spring and lateral springs, respectively, given in units of newton seconds per meter. The effects of the viscous damping on the band gaps are calculated and the results are shown in Figs. 10 and 11.

Fig. 10 shows how linear viscous damping of the vertical spring c_1 can affect band gaps with $c_2 = 0$. It can be seen that the FRFs in the two band gaps change little as c_1 increases, whereas response peaks outside the band gaps are decreased. The greater the linear viscous damping is, the lower are the response peaks outside the band gaps. From these results, we can conclude that viscous damping of the vertical springs has little influence on the interval of band gaps but can reduce the peaks and smooth the frequency response curve outside the band gaps.

Fig. 11 shows the effect of the linear viscous damping of the lateral springs c_2 on the band gaps with $c_1 = 0$. Firstly, the first band gap and its lateral responses do not change as c_2 increases. Secondly, the second band gap is broadened, and its frequency

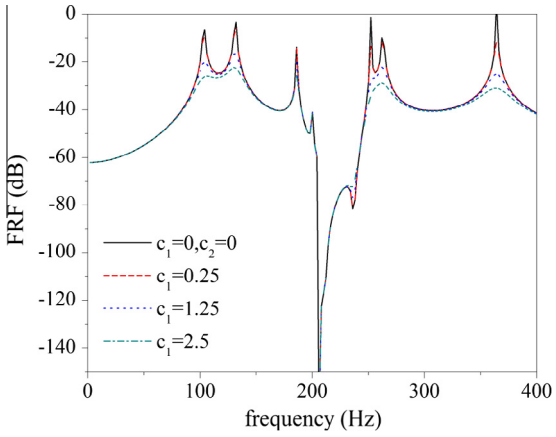

Fig. 10. Effect of damping of the vertical spring on band gaps.

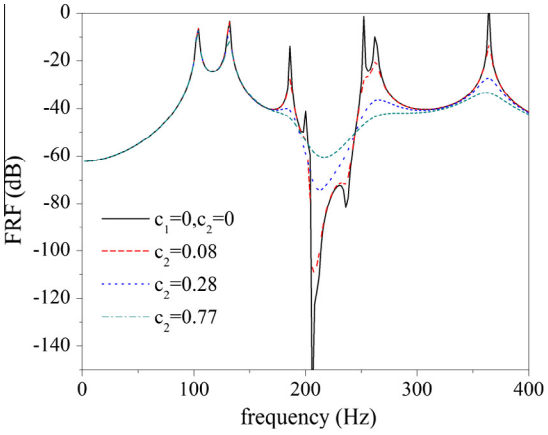

Fig. 11. Effect of damping of the lateral springs on band gaps.

responses are closer to those of the first band gap. The peaks and slopes of the frequency response curve are weakened significantly as the viscous damping increases. However, the attenuation within the second band gap is weakened. In a word, increasing the viscous damping of the lateral springs may broaden the second band gap

and reduce the vibration amplitude in specific frequency ranges. However, excessive viscous damping may deactivate the second band gap effect. Thus the second band gap can be tailored by the viscous damping according to the requirements of specific engineering applications.

Linear viscous damping from different parts of the system has various effects on the band gaps and the responses. Linear viscous damping of the vertical spring helps to smooth and lower the responses outside the band gaps but has little influence on either of the band gaps. On the other hand, linear viscous damping of the lateral springs can broaden the second band gap and lower the responses in specific frequency ranges with the loss of the attenuation within the second band gap. Damping from the LLR substructure is important in vibration suppression and noise absorption by virtue of its tailoring function in the band gaps.

5. Conclusion

The paper presents a comprehensive study of the flexural wave suppression of an acoustic metamaterial plate with negative Young's modulus substructure. It includes deriving analytical dispersion surfaces, effective mass density based on classical thin plate theory and conducting frequency response analysis by means of plane wave propagation and finite element method. The metamaterial plate can generate two low-frequency band gaps with relatively large frequency ranges and the effective mass density becomes negative within the band gaps. The key working mechanism for the metamaterial plate with LLR substructures is that the four-link mechanism transforms the flexural wave into a longitudinal wave and the resonance stores energy and blocks the wave within the second band gap. The effect of the geometry parameter of the lateral substructure is also studied and we conclude that varying the ratio of the horizontal and vertical distances can flexibly tune the band gaps. Damping from different springs has different effects on the band gaps. However, damping could smooth and lower the responses in the higher frequency range outside the second band gap but has little influence on the first band gap. The damping from the lateral resonators helps to broaden the second band gap but weakens the band gap effect. Finally, the combination of the LLR substructure and the metamaterial plate can be used in vibration suppression and noise absorption.

Acknowledgement

The first author is grateful for sponsorship from the China Scholarship Council.

References

[1] Peng H, Pai PF. Design of multi-stopband metamaterial plates for absorption of broadband elastic waves and vibration; 2015. p. 94380X.
[2] Wang T, Sheng MP, Guo HB. Multi-large low-frequency band gaps in a periodic hybrid structure. Mod Phys Lett B 2016;30:1650116.
[3] Huang HH, Sun CT, Huang GL. On the negative effective mass density in acoustic metamaterials. Int J Eng Sci 2009;47:610–7.
[4] Huang GL, Sun CT. Band gaps in a multiresonator acoustic metamaterial. J Vib Acoust 2010;132:031003.
[5] Huang HH, Sun CT. Theoretical investigation of the behavior of an acoustic metamaterial with extreme Young's modulus. J Mech Phys Solid 2011;59:2070–81.
[6] Pope SA, Daley S. Viscoelastic locally resonant double negative metamaterials with controllable effective density and elasticity. Phys Lett 2010;374:4250–5.
[7] Chang Z, Guo H-Y, Li B, Feng X-Q. Disentangling longitudinal and shear elastic waves by neo-Hookean soft devices. Appl Phys Lett 2015;106:161903.
[8] Yu D, Liu Y, Wang G, Zhao H, Qiu J. Flexural vibration band gaps in Timoshenko beams with locally resonant structures. J Appl Phys 2006;100:124901.
[9] Liu Y, Yu D, Li L, Zhao H, Wen J, Wen X. Design guidelines for flexural wave attenuation of slender beams with local resonators. Phys Lett 2007;362:344–7.
[10] Sun H, Du X, Pai PF. Theory of metamaterial beams for broadband vibration absorption. J Intell Mater Syst Struct 2010.
[11] Pai PF, Peng H, Jiang S. Acoustic metamaterial beams based on multi-frequency vibration absorbers. Int J Mech Sci 2014;79:195–205.
[12] Gusev VE, Wright OB. Double-negative flexural acoustic metamaterial. New J Phys 2014;16:123053.
[13] Boutin C, Roussillon P. Wave propagation in presence of oscillators on the free surface. Int J Eng Sci 2006;44:180–204.
[14] Strasberg M, Feit D. Vibration damping of large structures induced by attached small resonant structures. J Acoust Soc Am 1996;99:335–44.
[15] Schwan L, Boutin C, Padrón LA, Dietz MS, Bard P-Y, Taylor C. Site-city interaction: theoretical, numerical and experimental crossed-analysis. Geophys J Int 2016.
[16] Schwan L, Boutin C, Dietz M, Padron L, Bard P-Y, Ibraim E, et al. Multi-building interactions and site-city effect: an idealized experimental model. In: Experimental research in earthquake engineering. Springer; 2015. p. 459–76.
[17] Peng H, Pai P Frank. Acoustic metamaterial plates for elastic wave absorption and structural vibration suppression. Int J Mech Sci 2014;89:350–61.
[18] Chronopoulos D, Antoniadis I, Collet M, Ichchou M. Enhancement of wave damping within metamaterials having embedded negative stiffness inclusions. Wave Motion 2015;58:165–79.
[19] Sun C, Chen J. Dynamic behavior of sandwich beam with internal resonators. In: J Sandw Struct Mater. p. 391–408.
[20] Chen J, Sharma B, Sun C. Dynamic behaviour of sandwich structure containing spring-mass resonators. Compos Struct 2011;93:2120–5.
[21] Sharma B, Sun C. Impact load mitigation in sandwich beams using local resonators. J Sandw Struct Mater 2015.
[22] Takahashi D, Tanaka M. Flexural vibration of perforated plates and porous elastic materials under acoustic loading. J Acoust Soc Am 2002;112:1456–64.
[23] Yang Z, Mei J, Yang M, Chan NH, Sheng P. Membrane-type acoustic metamaterial with negative dynamic mass. Phys Rev Lett 2008;101:204301.
[24] Nouh M, Aldraihem O, Baz A. Vibration characteristics of metamaterial beams with periodic local resonances. J Vib Acoust 2014;136:061012.
[25] Nouh M, Aldraihem O, Baz A. Wave propagation in metamaterial plates with periodic local resonances. J Sound Vib 2015;341:53–73.
[26] Chesnais C, Boutin C, Hans S. Effects of the local resonance in bending on the longitudinal vibrations of reticulated beams. Wave Motion 2015;57:1–22.
[27] Chesnais C, Boutin C, Hans S. Effects of the local resonance on the wave propagation in periodic frame structures: generalized Newtonian mechanics. J Acoust Soc Am 2012;132:2873–86.
[28] Huang HH, Sun CT. Anomalous wave propagation in a one-dimensional acoustic metamaterial having simultaneously negative mass density and Young's modulus. J Acoust Soc Am 2012;132:2887–95.
[29] Su Y, Sun C. Design of double negativity elastic metamaterial. Int J Smart Nano Mater 2015;6:61–72.
[30] Qin QH. Hybrid-Trefftz finite element method for Reissner plates on an elastic foundation. Comput Methods Appl Mech Eng 1995;122:379–92.
[31] Graff KF. Wave motion in elastic solids. Dover Publications.
[32] Qin QH. Transient plate bending analysis by hybrid Trefftz element approach. Commun Numer Meth Eng 1996;12:609–16.
[33] Han L, Zhang Y, Li X-M, Jiang L-H, Chen D. Flexural vibration reduction of hinged periodic beam–foundation systems. Soil Dynam Earthq Eng 2015;79 (Part A):1–4.
[34] Qin QH. Trefftz finite element method and its applications. Appl Mech Rev 2005;58:316–37.
[35] Qin QH, Wang H. Matlab and C programming for Trefftz finite element methods. CRC Press; 2008.